

Femtosecond Spectroscopic Study of MLCT Excited-State Dynamics of Cr(CO)₄(bpy): Excitation-Energy-Dependent Branching between CO Dissociation and Relaxation

Ian R. Farrell,[†] Pavel Matousek,[‡] and Antonín Vlček, Jr.,^{*,‡}

Contribution from the Department of Chemistry, Queen Mary and Westfield College, University of London, London E1 4NS, United Kingdom, and Central Laser Facility, CLRC, Rutherford Appleton Laboratory, Chilton, Didcot, Oxfordshire OX11 0QX, United Kingdom

Received December 15, 1998. Revised Manuscript Received April 6, 1999

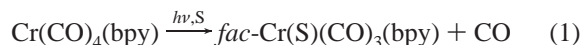
Abstract: The excited-state dynamics of Cr(CO)₄(bpy) were studied with pump–probe time-resolved absorption spectroscopy in pyridine and CH₂Cl₂ solutions. Samples were excited into the strong Cr → bpy metal-to-ligand charge-transfer (MLCT) absorption band by tunable laser pulses. It was found that the Cr(S)(CO)₃-(bpy) photoproduct (S = solvent) is formed completely within the time resolution of the experiment, that is ca. 600 fs, parallel with the population of two unreactive excited states which act as excitation energy traps. The photoproduct does not undergo any changes during the time range investigated (0–2 ns), while the two “trapping states” decay, in pyridine, with lifetimes of 8 and 87 ps, respectively. Branching of the evolution of the optically prepared Franck–Condon MLCT state between the reactive and relaxation channels is highly dependent on the excitation energy and limits the photochemical quantum yield of CO dissociation. The course and outcome of the photochemistry of Cr(CO)₄(bpy), and of many analogous MLCT-active organometallic compounds, is obviously determined at the earliest times after optical excitation. In addition to the excited-state dynamics, the reorientation time of ground-state Cr(CO)₄(bpy) molecules was measured to be 32 ps in pyridine at room temperature.

Introduction

Although traditionally deemed¹ photochemically inert, many organometallic compounds with low-lying metal-to-ligand charge-transfer (MLCT) excited states exhibit a unique photoreactivity.^{2,3} Irradiation into their MLCT absorption bands often causes splitting of a metal–ligand, metal–metal, or intraligand bond. Photochemical isomerizations, oxidative additions, or ionizations caused by MLCT excitations are also known.³ The photochemistry of organometallic α -diimine complexes, namely carbonyl diimines and alkyl diimines, is especially interesting. MLCT excitation often leads to CO dissociation or homolytic splitting of a metal–alkyl bond, respectively.^{2,4–16} Since highly reactive, coordinatively unsaturated Lewis acidic or radical metal complexes are produced, these

reactions can be used as first steps of photocatalytic cycles and photoinitiated processes. Their dynamics are of great fundamental scientific interest.^{2,6} The mechanism of photochemical dissociation of a CO ligand from carbonyl diimine complexes of first-row transition metals is intriguing since the CO ligand, although being just a spectator in the M → diimine MLCT excitation, appears to dissociate directly from the optically prepared Franck–Condon excited state, without an intervention of any intermediate excited state.^{2,5,6}

Dissociation of a CO ligand from the Cr(CO)₄(bpy) complex (Figure 1) is a typical example of such a behavior.^{2,5–7,17–20} Irradiation into its intense MLCT absorption band causes dissociation of an axial CO ligand, which is replaced by a solvent molecule, S, or by any potential ligand (e.g., phosphine) present in solution:



The dissociative mechanism of reaction 1 was clearly demon-

[†] University of London.

[‡] CLRC Rutherford Appleton Laboratory.

(1) Geoffroy, G. L.; Wrighton, M. S. *Organometallic Photochemistry*; Academic Press: New York, 1979.

(2) Vlček, A., Jr. *Coord. Chem. Rev.* **1998**, *177*, 219.

(3) Vogler, A.; Kunkely, H. *Coord. Chem. Rev.* **1998**, *177*, 81.

(4) Stufkens, D. J. *Coord. Chem. Rev.* **1990**, *104*, 39.

(5) Vichová, J.; Hartl, F.; Vlček, A., Jr. *J. Am. Chem. Soc.* **1992**, *114*, 10903.

(6) Vlček, A., Jr.; Vichová, J.; Hartl, F. *Coord. Chem. Rev.* **1994**, *132*, 167.

(7) Virrels, I. G.; George, M. W.; Turner, J. J.; Peters, J.; Vlček, A., Jr. *Organometallics* **1996**, *15*, 4089.

(8) van Dijk, H. K.; Stufkens, D. J.; Oskam, A. *J. Am. Chem. Soc.* **1989**, *111*, 541.

(9) Johnson, C. E.; Trogler, W. C. *J. Am. Chem. Soc.* **1981**, *103*, 6352.

(10) Stufkens, D. J.; Aarnts, M. P.; Rossenaar, B. D.; Vlček, A., Jr. *Pure Appl. Chem.* **1997**, *69*, 831.

(11) Stufkens, D. J.; Aarnts, M. P.; Nijhoff, J.; Rossenaar, B. D.; Vlček, A., Jr. *Coord. Chem. Rev.* **1998**, *171*, 93.

(12) Stufkens, D. J.; Vlček, A., Jr. *Coord. Chem. Rev.* **1998**, *177*, 127.

(13) Rossenaar, B. D.; Stufkens, D. J.; Oskam, A.; Fraanje, J.; Goubitz, K. *Inorg. Chim. Acta* **1996**, *247*, 215.

(14) Rossenaar, B. D.; George, M. W.; Johnson, F. P. A.; Stufkens, D. J.; Turner, J. J.; Vlček, A., Jr. *J. Am. Chem. Soc.* **1995**, *117*, 11582.

(15) Rossenaar, B. D.; Kleverlaan, C. J.; van de Ven, M. C. E.; Stufkens, D. J.; Vlček, A., Jr. *Chem. Eur. J.* **1996**, *2*, 228.

(16) Kleverlaan, C. J.; Stufkens, D. J.; Clark, I. P.; George, M. W.; Turner, J. J.; Martino, D. M.; van Willigen, H.; Vlček, A., Jr. *J. Am. Chem. Soc.* **1998**, *120*, 10871.

(17) Balk, R. W.; Snoeck, T.; Stufkens, D. J.; Oskam, A. *Inorg. Chem.* **1980**, *19*, 3015.

(18) Wieland, S.; Reddy, K. B.; van Eldik, R. *Organometallics* **1990**, *9*, 1802.

(19) Fu, W. F.; van Eldik, R. *Inorg. Chim. Acta* **1996**, *251*, 341.

(20) Fu, W.-F.; van Eldik, R. *Inorg. Chem.* **1998**, *37*, 1044.

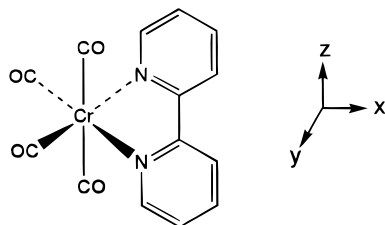


Figure 1. Schematic structure of $\text{Cr}(\text{CO})_4(\text{bpy})$ and chosen orientation of axes.

strated by measuring positive values of activation volumes at several irradiation wavelengths.^{18–20} Importantly, the quantum yield was found to decrease with increasing irradiation wavelength across the region of the visible MLCT absorption band.^{5,6} This observation clearly demonstrated that the reacting state has a memory of the original excitation, effectively ruling out any relaxation into a thermally equilibrated state prior to the CO dissociation. Accordingly, *fac*- $\text{Cr}(\text{S})(\text{CO})_3(\text{bpy})$ is the only photoproduct species detected in the nanosecond time domain by time-resolved IR and UV–vis absorption spectroscopy following nanosecond laser pulse excitation of $\text{Cr}(\text{CO})_4(\text{bpy})$ in CH_2Cl_2 or pyridine solution.⁷ No evidence of any long-lived MLCT excited state was obtained. An early picosecond spectroscopic study of reaction 1 indicated⁵ that two species are produced within the 30 ps laser pulse, one short-lived (<100 ps) and the other persistent on the time scale of the experiment, up to 10 ns. Comparison between picosecond and nanosecond absorption spectra later enabled⁷ the characterization of the long-lived species as the *fac*- $\text{Cr}(\text{S})(\text{CO})_3(\text{bpy})$ photoproduct, while the nature of the short-lived transient remained unclear.²¹ This experiment gave an estimate of the lower limit of the CO dissociation rate constant as $3 \times 10^{10} \text{ s}^{-1}$, but the initial MLCT excited-state dynamics responsible for the CO ligand dissociation remained obscure.

The photochemistry of $\text{Cr}(\text{CO})_4(\text{bpy})$ is being studied as a prototypical case of prompt CO dissociation from MLCT excited state. It is expected that a detailed elucidation of its mechanism will unravel general principles applicable to the photochemistry of more complex organometallic systems. Herein, we have investigated the MLCT photochemistry and excited-state relaxation of $\text{Cr}(\text{CO})_4(\text{bpy})$ with a time resolution of about 400 fs. This research is aimed especially at the elucidation of the mechanism of CO dissociation from an MLCT excited state, the estimation of its rate, and the understanding of the factors that limit its quantum yield.

Experimental Section

$\text{Cr}(\text{CO})_4(\text{bpy})$ was prepared by the method of Stiddard²² and purified by recrystallization from a CH_2Cl_2 /isooctane mixture under a nitrogen atmosphere. Its purity was checked by IR, UV–vis, and ^1H NMR spectroscopies. Pyridine, CH_2Cl_2 , and acetonitrile solvents of spectroscopic grade were obtained from Aldrich.

The femtosecond absorption spectrometer used is described in detail elsewhere.^{23–25} The excitation and probe pulses (200–250 μm diameter) overlapped in a slightly noncollinear (10°) geometry on a 0.5 or 2 mm cell through which the sample solution was circulated. Tunable excitation laser pulses of a width of ca. 250 fs were derived from an optical parametric amplifier (OPA) operating in a femtosecond mode

(21) Our early picosecond study⁵ has revealed the presence of two transients, called “fast” and “slow”, the former decaying within 200 ps and the latter being essentially persistent. Comparison of these transients with those characterized later⁷ by nanosecond TRIR spectroscopy showed that the “slow” transient is, in fact, the *fac*- $\text{Cr}(\text{S})(\text{CO})_3(\text{bpy})$ photoproduct, while the “fast” one corresponds to the trapping states fully unraveled and examined herein.

(22) Stiddard, M. H. B. *J. Chem. Soc.* **1962**, 4712.

at a repetition rate of 1 kHz. The pulse energy was in the range 1–3 μJ . The OPA was pumped by 400 nm laser pulses, generated by frequency-doubling the amplified 800 nm fundamental output of a Ti:sapphire regenerative amplifier. In some experiments, the sample was excited directly with the 400 nm pulses, bypassing the OPA. The excitation beam was chopped mechanically at a frequency of ca. 200 Hz. Kinetic profiles at a single monitoring wavelength were measured using probe pulses obtained by selecting a portion of a white light continuum with 10-nm band-pass interference filters. The continuum was generated in D_2O by a part of the 800 nm fundamental laser beam. To monitor kinetic traces at 800 nm, the fundamental pulses of the regenerative amplifier were used as the probe beam. The delay time between the probe and excitation beams was selected by an optical delay line. The probe beam was split into sample and reference beams, the latter bypassing the sample cell. Their intensities were monitored using two photodiodes to obtain both sample and reference signals, with and without excitation, respectively. An analogue ratio of the photodiode signals was obtained and fed into a lock-in amplifier. Signals were accumulated at each delay time for 5 s. To reduce any systematic errors due to sample degradation, long-term laser power changes, etc., the delay time values were sampled at least 10 times in a random order. The data were processed to give the difference between the sample absorbance measured with and without the laser excitation (ΔA) as a function of the delay time. Fitting of the experimental kinetics was performed with Microcal Origin version 5.0 software.

Time-resolved spectra in the 560–720 nm range were obtained by passing the white light continuum through the excited sample before dispersing it spectrally onto two 512 pixel diode array detectors. The signal was processed on a PC to give the absorbance difference at individual wavelengths (pixels), without using lock-in amplification.²⁵

Ultrafast spectroscopic measurements were performed on flowing, degassed solutions whose absorbance at the excitation wavelength was kept in the range 0.6–1.0. The solution was kept in the dark during measurements. The extent of unavoidable sample photodecomposition on the cell surface by the laser excitation was minimized by slightly defocusing the excitation beam when necessary or, in the case of 400 nm excitation, by diminishing its intensity with a gray filter of 0.6 optical density. Net sample photodecomposition during the measurements was checked by UV–vis absorption spectroscopy and found to be negligible. ΔA values measured immediately after excitation were in the range 8×10^{-3} – 5×10^{-2} .

To estimate the time resolution of the instrument, we have used $[\text{Ru}(\text{bpy})_3]^{2+}$ in acetonitrile solution as a standard. The long-lived excited-state absorption of $[\text{Ru}(\text{bpy})_3]^{2+}$ is known to be fully developed within the first 300 fs after excitation.²⁶ Assuming that the instrument time resolution is longer than 300 fs, the kinetic profiles of the rise of the $[\text{Ru}(\text{bpy})_3]^{2+}$ excited-state absorption correspond to the integrated instrument response function. These measurements were performed at several different monitoring and excitation wavelengths, all leading to a conservative estimate of the instrument time resolution as 600 fs (see inset of Figure 5). To determine the actual time resolution, simulations of a convoluted 600 fs Gaussian response function with various exponentially rising signals were performed. It followed that rise times of 400 fs and longer could be resolved with the current experimental setup.

Results

$\text{Cr}(\text{CO})_4(\text{bpy})$ shows an intense absorption band in the visible spectral region which has been attributed to the allowed $d_{xz} \rightarrow \pi^*(\text{bpy})$ MLCT transition.^{4,17,27,28} In pyridine solution, this band occurs at 493 nm ($\epsilon = 3680 \text{ M}^{-1} \text{ cm}^{-1}$), while it is slightly

(23) Matousek, P.; Parker, A. W.; Taday, P. F.; Toner, W. T.; Towrie, M. *Opt. Commun.* **1996**, *127*, 307.

(24) Towrie, M.; Parker, A. W.; Shaikh, W.; Matousek, P. *Meas. Sci. Technol.* **1998**, *9*, 816.

(25) Towrie, M.; Matousek, P.; Parker, A. W.; Jackson, S.; Bisby, R. H. Rutherford Appleton Laboratory Report, 1997, p 183.

(26) Damrauer, N. H.; Cerullo, G.; Yeh, A.; Boussie, T. R.; Shank, C. V.; McCusker, J. K. *Science* **1997**, *275*, 54.

(27) Guillaumont, D.; Daniel, C.; Vlček, A., Jr. *Inorg. Chem.* **1997**, *36*, 1684.

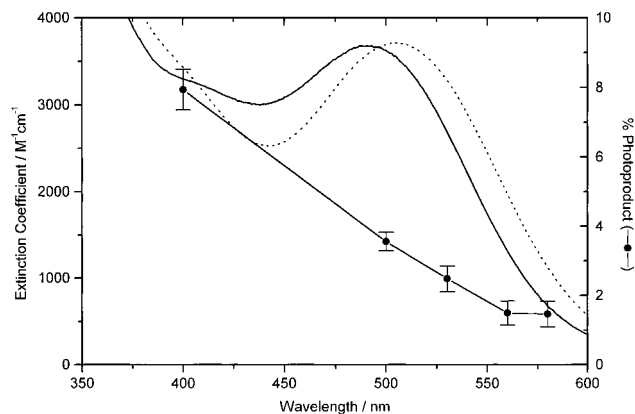


Figure 2. Absorption spectra of $\text{Cr}(\text{CO})_4(\text{bpy})$ in pyridine (—) and CH_2Cl_2 (···) solutions, shown together with the photoproduct contribution to the initial ($t = 0$) transient absorption, C_0 , measured at various excitation wavelengths (●).

broader and red-shifted in CH_2Cl_2 (506 nm, $3715 \text{ M}^{-1} \text{ cm}^{-1}$), see Figure 2. Pyridine affords the largest spectral window for the time-resolved visible absorption experiments and was therefore used as a solvent in most of the experiments described herein. For comparison, several kinetic profiles were also measured in CH_2Cl_2 . The quality of the ultrafast spectroscopic data obtained from pyridine solutions was always much higher than that from CH_2Cl_2 .

Time-resolved absorption spectra of $\text{Cr}(\text{CO})_4(\text{bpy})$ in pyridine were measured in the spectral range 560–720 nm using diode array detection, see Figure 3. Spectra obtained at early times after 500 nm excitation (2, 3, and 20 ps) show a broad absorption, extending over the whole spectral range studied, with apparent maxima at about 590 and 700 nm. This broad absorption decays with time, leaving a well-developed absorption band which peaks at about 660 nm (see the spectrum obtained at 400 ps). The intensity of this band is constant on the time scale of this experiment, i.e., until 1 ns. The persistence of this absorption band, together with the similarity of its shape and position to that observed in the nanosecond time domain,⁷ show that it belongs to the *fac*- $\text{Cr}(\text{S})(\text{CO})_3(\text{bpy})$ photoproduct. This species has already been characterized by nanosecond TRIR spectroscopy.⁷ The broad transient absorption that occurs immediately after excitation appears to be composed of the 660 nm photoproduct band and of a rapidly decaying transient absorption that extends to both longer and shorter wavelengths. This short-lived component is tentatively assigned to MLCT excited state(s) of $\text{Cr}(\text{CO})_4(\text{bpy})$. Generally, absorptions in the red/near-IR region and at wavelengths below 600 nm, which originate in the bpy^{*+} chromophore,²⁹ are typical of $\text{M} \rightarrow \text{bpy}$ MLCT states. The spectrum of the reduced $[\text{Cr}(\text{CO})_4(\text{bpy})]^{+}$ corroborates this assignment.⁵

Detailed kinetic information on the temporal evolution of the observed transients was obtained by measuring time profiles of transient absorbance at selected probe wavelengths. First, we shall discuss results obtained at various wavelengths in the range 620–800 nm, outside the region of the $\text{Cr}(\text{CO})_4(\text{bpy})$ ground-state absorption, and at 400 nm, where the transient absorption is much more intense than the bleach. Regardless of the probe wavelength (400, 620, 670, 690, 710, 757, or 800 nm), excitation caused a sharp rise in absorbance, followed by a double-exponential decay with a constant component. Two typical kinetic traces are shown in Figure 4. The experimental kinetics

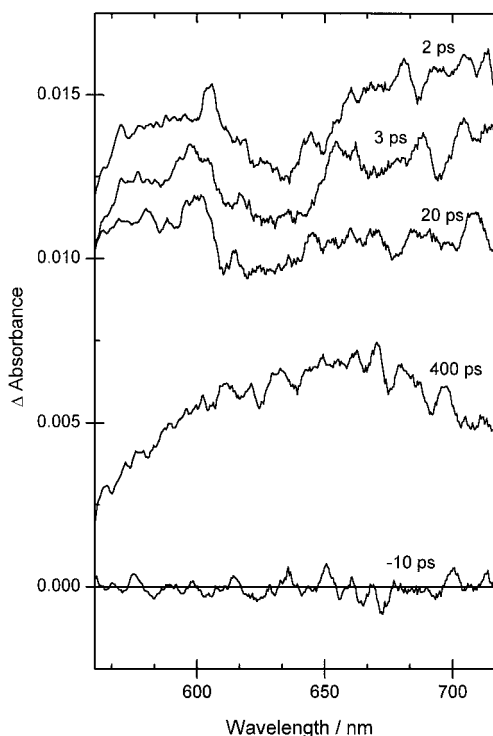


Figure 3. Time-resolved difference absorption spectra of $\text{Cr}(\text{CO})_4(\text{bpy})$ in pyridine at selected time delays after excitation. Measured with a diode array detection using a magic angle orientation of the polarization directions. From top to bottom, time delay was 2, 3, 20, and 400 ps. The -10 ps spectrum shows the baseline, measured 10 ps before excitation. Δ Absorbance is defined as the sample absorbance measured at a given time after excitation minus that before excitation. No correction for the spectral chirp (about 1.5 ps across the region studied) was made.

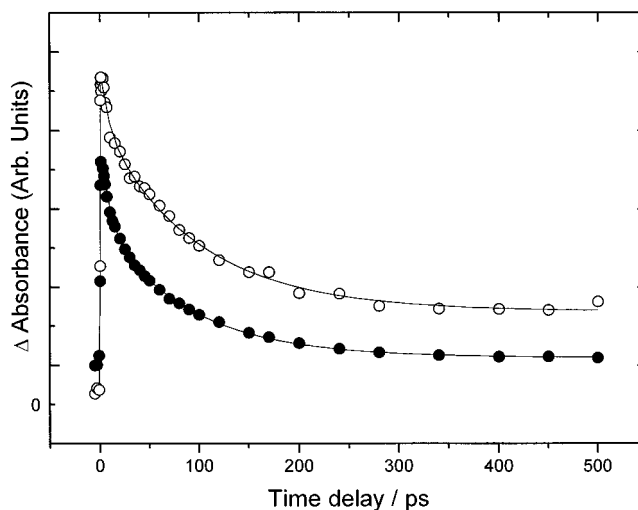


Figure 4. Kinetic profiles of the difference absorbance of $\text{Cr}(\text{CO})_4(\text{bpy})$ in pyridine following 500-nm laser pulse excitation. Top (○), monitored at 640 nm; bottom (●), monitored at 800 nm. Polarization directions of the excitation and probe beams contained a magic angle. (The leftmost experimental points at slightly negative time delays were measured before excitation.)

were found to fit very well to eq 2:

$$A = A_0 + A_1 \exp(-t/\tau_1) + A_2 \exp(-t/\tau_2) \quad (2)$$

The lifetimes of the two decay processes, τ_1 and τ_2 , are independent of the probe wavelength and of the excitation

(28) Vlček, A., Jr.; Grevels, F.-W.; Snoeck, T. L.; Stufkens, D. J. *Inorg. Chim. Acta* **1998**, 278, 83.

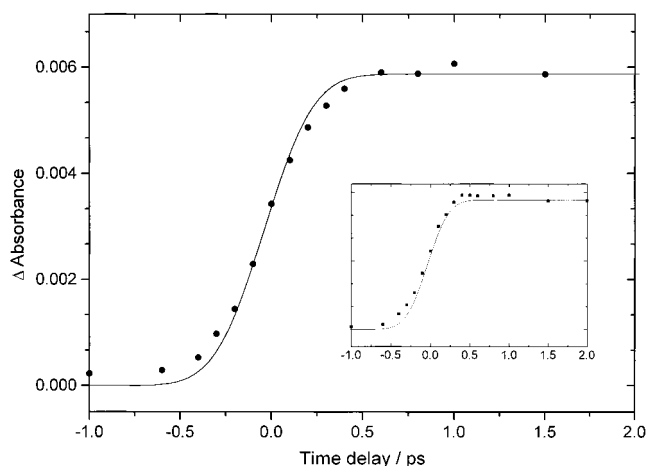
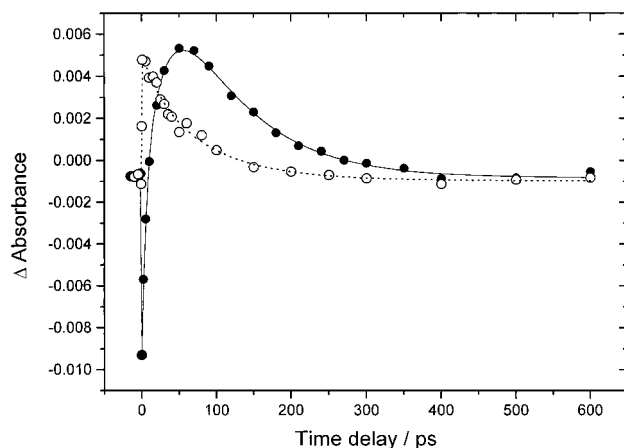
(29) Noble, B. C.; Peacock, R. D. *Spectrochim. Acta* **1990**, 46A, 407.

Table 1. Excitation Wavelength Dependence of the Excited-State Dynamics of $\text{Cr}(\text{CO})_4(\text{bpy})$ in Pyridine Solution at 293 K^a

λ_{exc} (nm)	E_{exc} (cm ⁻¹)	C_0 (%)	τ_1 (ps)	C_1 (%)	τ_2 (ps)	C_2 (%)
400	25 000	7.9	8.1	53.0	69.8	39.4
500	20 000	3.6	7.9	35.2	84.3	61.2
530	18 870	2.5	7.7	32.7	86.2	64.8
560	17 860	1.5	7.8	28.5	88.6	70.0
580	17 240	1.5	8.4	30.9	87.6	67.6

wavelength, the latter varied in the 500–580 nm range. Average values of 8 ± 1 and 87 ± 3 ps were measured, respectively. A smaller value of τ_2 , 70 ± 5 ps, was determined using excitation at 400 nm. The relative contributions C_i of individual kinetic components to the initially formed transient absorption (i.e., extrapolated to zero time delay) were estimated as $C_i = A_i/(A_0 + A_1 + A_2)$, $i = 0, 1, 2$. It was found that, under visible light excitation, the longer-lived 87 ps component dominates the initially formed transient absorption, accounting for 50–60%, while the 8 ps transient contributes about 15–35%, depending on the monitoring wavelength. The relative importance of these two transients is reversed under 400 nm excitation, for which the initial transient signal is dominated by the 8 ps component, which accounts for 53%. The relative contribution of the time-independent component C_0 , $A_0/(A_0 + A_1 + A_2)$, reflects the photoproduct absorption spectrum shown in Figure 3. The largest values of 28 and 27% were measured when probing at 620 and 670 nm, respectively, while they dropped on going to longer wavelengths: 21, 19, 14, and 3% at 690, 710, 757, and 800 nm, respectively. A contribution of only 8% was found when probing at 400 nm, where the MLCT excited-state absorption is expected⁵ to be stronger than that of the photoproduct. These results fully agree with the overall picture obtained from the time-resolved spectra shown in Figure 3. The constant component obviously corresponds to the $\text{Cr}(\text{S})(\text{CO})_3(\text{bpy})$ photoproduct, while the two decaying transients account for the broad MLCT excited-state absorption observed at early time delays. Changing the solvent from pyridine to CH_2Cl_2 has very little effect on the $\text{Cr}(\text{CO})_4(\text{bpy})$ excited-state dynamics. Again, a double-exponential decay with a constant component was observed after laser pulse excitation. In CH_2Cl_2 , the lifetimes of the decaying components, τ_1 and τ_2 , were determined as 15 ± 7 and 82 ± 10 ps, accounting for ca. 30 and 60%, of the initial absorption, respectively.

The quantum yield of the photochemical substitution (1) of a CO ligand in $\text{Cr}(\text{CO})_4(\text{bpy})$ by $\text{L} = \text{PPh}_3$ was shown⁵ to depend strongly on the excitation wavelength. An important question that arises is whether this relationship is mirrored by the dependence of excited-state dynamics on excitation wavelength. To answer this question, kinetic profiles of the transient absorption at 800 nm were measured as a function of the excitation wavelength. The results are summarized in Table 1 and Figure 2. It follows that the overall behavior is qualitatively the same at all the excitation wavelengths examined. However, the relative contribution of the $\text{Cr}(\text{S})(\text{CO})_3(\text{bpy})$ photoproduct absorption to the initially formed transient, C_0 , decreases with increasing excitation wavelength throughout the region of the MLCT absorption, apparently leveling off in its long-wavelength onset, see Figure 2. This excitation wavelength dependence was further confirmed by the kinetic traces of the absorbance at 620 nm, which show a 1.6-fold drop in C_0 upon changing excitation from 400 to 500 nm. Similarly, kinetic profiles obtained at 649 nm in CH_2Cl_2 using four different excitation wavelengths in the range 500–580 nm show that, while the two decay lifetimes, τ_1 and τ_2 , do not depend on the excitation wavelength, the contribution of the photoproduct to the initial transient absorp-

**Figure 5.** Kinetic profile of the rise of the transient absorption at 800 nm of $\text{Cr}(\text{CO})_4(\text{bpy})$ in pyridine following 500 nm laser pulse excitation (●). The sigmoidal curve (—) is the integrated instrument response function determined by the rise in excited-state absorption of $[\text{Ru}(\text{bpy})_3]^{2+}$ in acetonitrile, as shown in the inset.**Figure 6.** Kinetic profile of the difference absorbance of $\text{Cr}(\text{CO})_4(\text{bpy})$ in pyridine following 500 nm laser pulse excitation, monitored at 530 nm, i.e., in the region of ground-state absorption. (—, ●): Parallel orientation of the polarization directions of the excitation and probe beams. (···, ○): Magic angle orientation.

tion decreases from ca. 13% when excited at 500 and 530 nm to 7% under 560 and 580 nm excitations.

The initial, sharp rise of the $\text{Cr}(\text{CO})_4(\text{bpy})$ transient absorption was analyzed in detail in order to unravel any possible formation kinetics. The absorbance was found to be fully developed within the first 600 fs after excitation, regardless of the probe or excitation wavelength or the solvent used, pyridine or CH_2Cl_2 . The kinetic profiles obtained on a short time scale for $\text{Cr}(\text{CO})_4(\text{bpy})$ follow well the integrated instrument response curve, determined using $[\text{Ru}(\text{bpy})_3]^{2+}$, see Figure 5. It follows that the initial excited-state dynamics of $\text{Cr}(\text{CO})_4(\text{bpy})$, which lead to CO dissociation and to the population of unreactive MLCT excited states, are complete within the instrument response time, that is within 600 fs, its rise time thus being shorter than 400 fs, see the Experimental Section.

An intriguing kinetic behavior was found when the absorbance was monitored in the spectral region where the ground-state $\text{Cr}(\text{CO})_4(\text{bpy})$ absorbs. Again, the same type of kinetic profile was obtained regardless the solvent (pyridine or CH_2Cl_2) or the excitation wavelength: 500, 530, or 560 nm. Typical results obtained in pyridine solution are shown in Figure 6. Kinetic curves obtained using the perpendicular or magic angle

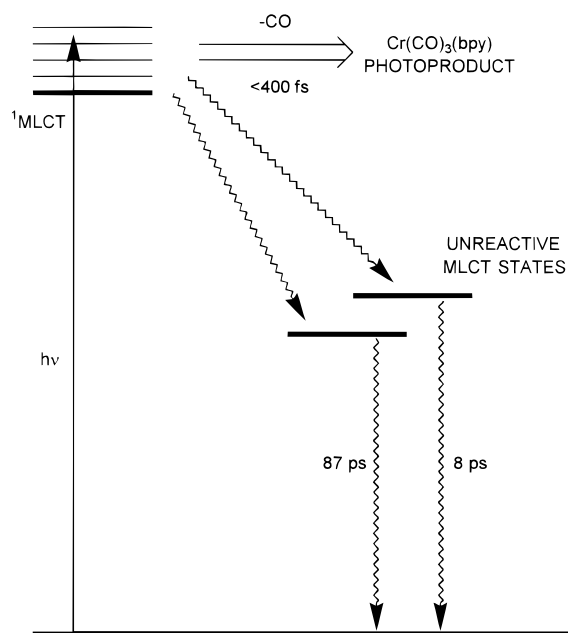
(54.7°) polarization orientations of the excitation and probe beams show the expected double-exponential decay kinetics with a constant component. The latter is slightly negative since the bleached ground-state absorption prevails over the photoproduct absorption. However, a different kinetic picture was obtained if the pump and probe beams were polarized in the same direction: excitation caused an instantaneous drop in the solution absorbance, manifested by a large negative signal, see Figure 6. This bleached absorbance then recovered with a lifetime of 32 ± 2 ps, reaching a positive maximum before decaying with a lifetime of ca. 90 ps to leave a constant, negative component. The same behavior was found in CH_2Cl_2 with a recovery lifetime of 15 ± 2 ps. (The latter value is just a rough estimate since the data fitting was complicated by the nearly identical τ_1 value.) This behavior can be explained by the simultaneous decay of the photoproduct, positive transient absorption and the recovery of the negative bleached ground-state absorption. Because the MLCT transition of $\text{Cr}(\text{CO})_4(\text{bpy})$ is strongly polarized,⁴ excitation causes a selective depletion of those $\text{Cr}(\text{CO})_4(\text{bpy})$ molecules whose C_2 symmetry axis (i.e., x) is oriented parallel to the polarization direction of the excitation laser pulse. (See Figure 1 for the chosen axes orientation.) A probe beam polarized parallel to excitation pulse is not absorbed by the remaining $\text{Cr}(\text{CO})_4(\text{bpy})$ molecules of different orientations, and a strong negative difference absorption signal arises immediately after excitation. On a longer time scale, reorientation of the ground-state $\text{Cr}(\text{CO})_4(\text{bpy})$ molecules replenishes the population of the parallel oriented molecules with a reorientation time constant of 32 ps. Hence, the bleached absorption recovers and the overall signal becomes positive, due to the still present absorption by the unreactive, but decaying, excited state. The subsequent absorption decay is identical to that found at longer probe wavelengths, out of the bleach region, i.e., approximately 90 ps. The assignment of the bleach recovery to the ground-state molecular reorientation is consistent with the 2-fold decrease of its time constant on going from pyridine to CH_2Cl_2 , whose viscosity is 2.3 times smaller. The bleaching of the $\text{Cr}(\text{CO})_4(\text{bpy})$ ground-state absorption and its subsequent recovery are not observed if the polarization of the probe beam is perpendicular to that of the excitation pulse. This is simply because the probe beam is absorbed by the remaining unexcited $\text{Cr}(\text{CO})_4(\text{bpy})$ molecules and does not detect the orientation-dependent hole in their population.

The kinetic profiles of the transient absorbance measured at wavelengths outside the region of the ground-state absorption ($\lambda_{\text{probe}} \geq 620$ nm) do not depend on the relative orientation of the excitation and probe beams, viz., parallel, perpendicular, or magic angle. The absence of the 32 ps (or similar) reorientation time in the excited-state dynamics implies that the excited-state and photoproduct absorptions are largely depolarized.

Discussion

The time-resolved spectra and kinetic behavior discussed above demonstrate that the dissociation of a CO ligand under visible or near-UV excitation of $\text{Cr}(\text{CO})_4(\text{bpy})$ occurs directly from the optically prepared $d_{xz} \rightarrow \pi^*(\text{bpy})$ $^1\text{MLCT}$ state, without an involvement of any intermediate state. This conclusion agrees with the results of the study of the excitation wavelength dependence of corresponding photochemical quantum yields.^{5,6} Importantly, the femtosecond experiments show that the Franck–Condon $d_{xz} \rightarrow \pi^*(\text{bpy})$ $^1\text{MLCT}$ excited state of $\text{Cr}(\text{CO})_4(\text{bpy})$ undergoes two parallel processes: CO dissociation and a nonradiative relaxation into two, lower-lying, unreactive excited states (see Scheme 1). These states, which decay with lifetimes

Scheme 1. Excited-State Dynamics of $\text{Cr}(\text{CO})_4(\text{bpy})$



of 8 and 87 ps, act as traps since their population prevents the CO loss. The branching between concurrent reactive and relaxation channels is fully complete within the first 600 fs after excitation, taking place with a time constant of 400 fs or shorter.

The observation that the $\text{Cr}(\text{S})(\text{CO})_3(\text{bpy})$ photoproduct is formed together with the trapping states on a time scale shorter than 400 fs implies that branching between the CO dissociation and relaxation occurs at the level of the optically prepared $d_{xz} \rightarrow \pi^*$ $^1\text{MLCT}$ Franck–Condon excited state. Remarkably, the corresponding branching ratio decreases across the spectral region of the MLCT absorption with decreasing excitation energy. This was manifested by the dependence of the photoproduct contribution to the initially formed transient absorption, C_0 , on the excitation wavelength, see Figure 2 and Table 1. It follows that the probabilities of the Franck–Condon state evolving along the dissociation and relaxation coordinates are strongly dependent on the particular vibronic level populated, which, in turn, is determined by the excitation energy used. Importantly, the branching ratio depends on the excitation energy in the same way as the photochemical quantum yield.⁵ This observation shows that the overall photochemical quantum yield of the CO dissociation from $\text{Cr}(\text{CO})_4(\text{bpy})$ is determined by the branching ratio, that is, by the probability of the evolution of the Franck–Condon state along the dissociative pathway that occurs in competition with the population of the unreactive trapping states.

In principle, the quantum yield could be further diminished by a geminate recombination of the photoproduct $\text{Cr}(\text{CO})_3(\text{bpy})$ fragment with CO. Since no spectroscopic evidence for such a recombination has been found, it is either absent or fully completed within the first 600 fs. This possibility cannot be excluded, since an analogous geminate recombination of the $\text{Cr}(\text{CO})_5$ species, photogenerated from $\text{Cr}(\text{CO})_6$, with CO occurs already on a time scale of 300 fs.³⁰

Changing the excitation wavelength from visible (500–580 nm) to near-UV (400 nm) not only more than doubles the relative contribution of the photoproduct to the initial signal but also reverses the relative contributions of the two trapping

(30) Lian, T.; Bromberg, S. E.; Asplund, M. C.; Yang, H.; Harris, C. B. *J. Phys. Chem.* **1996**, *100*, 11994.

states (Table 1). Inspection of the absorption spectra shown in Figure 2, together with the results of recent quantum chemical calculations,^{27,31} suggests that 400 nm irradiation simultaneously excites the $d_{xz} \rightarrow \pi^*$ MLCT and more energetic $\text{Cr} \rightarrow \text{CO}$ and higher $d \rightarrow 2,3\pi^*(\text{bpy})$ MLCT transitions. It follows that, while the relaxation of the $d_{xz} \rightarrow \pi^*$ ¹MLCT states leads preferentially to the long-lived trapping state (ca. 66%), the higher-lying states prepared by 400-nm excitation relax predominantly to the short-lived 8-ps state (53%), while the longer-lived one contributes only 39%. Apparently, the ratio in which the individual trapping states are populated depends on the electronic character of the Franck–Condon state. The shortening of the lifetime of the longer-lived trapping state from 87 to 70 ps on changing the excitation wavelength from the 500–580 nm region to 400 nm suggests a different character, either electronic or vibronic, of the trapping states populated from the $d_{xz} \rightarrow \pi^*$ and higher MLCT states.

The nature of the two trapping states cannot be assigned unequivocally on the basis of the data presented here. The most likely candidates are MLCT states whose orbital origin is different from the optically excited $d_{xz} \rightarrow \pi^*$ ¹MLCT one, especially the $d_{yz} \rightarrow \pi^*$ and $d_{x^2-y^2} \rightarrow \pi^*$ MLCT states, either spin singlets or triplets which have been calculated²⁷ as lying at lower energies. The $d_{xz} \rightarrow \pi^*$ ³MLCT state is also a possibility. The very existence of the two distinct decay kinetics (8 and 87 ps) implies that there is no equilibrium between the two trapping states. The observation of two short-lived excited states is in line with the very weak double emission known³² for $\text{Cr}(\text{CO})_4(\text{bpy})$. (The emission lifetime has not been reported, apparently being very short.) An alternative assignment of the trapping states to a $\text{Cr}(\text{CO})_4(\text{N-bpy})$ species, with one Cr–N bond broken, seems unlikely since bond re-formation is expected to take much longer than 90 ps. A possibility that the 8 ps transient decay reflects a dissipation of vibrational energy to the solvent^{33,34} was discarded on following grounds: (i) the near doubling of the lifetime on changing the solvent from pyridine to CH_2Cl_2 is not accompanied by a corresponding rise in thermal diffusivity,³³ which is ca. $9.1 \times 10^{-8} \text{ m}^2 \text{ s}^{-1}$ for both solvents, and (ii) vibrational cooling is expected to cause a narrowing or shifting of the excited-state absorption³⁴ instead of the uniform decay over the whole visible spectral region observed herein.

It is interesting to note that the real-time femtosecond study of the $\text{Cr}(\text{CO})_4(\text{bpy})$ excited-state dynamics fully confirms the inferences made from the excitation energy dependence of quantum yields obtained using continuous irradiation.⁵ The original conclusion, that the CO dissociation is ultrafast, occurring from the optically prepared ¹MLCT state which keeps the memory of the original excitation,⁵ has found a solid physical basis in the excitation energy dependence of the branching ratio between the initial excited-state processes. Compared with our early picosecond study of this system,⁵ the present experiments have shifted the upper limit of the time needed for the axial CO ligand to dissociate by 2 orders of magnitude, from some 30 ps to less than 400 fs, and unraveled the details of the MLCT excited-state dynamics, namely the population and decay of the trapping states. The observation of the genuinely ultrafast rate of CO dissociation poses, however, further questions of a fundamental interest, namely what is the physical origin of the

experimentally observed pressure^{18–20} and temperature⁵ effects on the quantum yield of $\text{Cr}(\text{CO})_4(\text{bpy})$ photosubstitution and of other ultrafast organometallic photoprocesses.^{8,16,35,36} While the pressure effects may be attributed to modifications of excited-state potential energy surfaces, the origin of the thermal activation is less clear and requires further investigation. Recent theoretical results, which indicate that quantum yields of photodissociation are higher when starting from a vibrationally excited ground state, could suggest possible explanation.^{37,38}

In conclusion, all the events which determine the quantum yield of the CO photodissociation from $\text{Cr}(\text{CO})_4(\text{bpy})$ were found to occur in a less than 400 fs after the MLCT excitation, i.e., with a rate constant larger than $2.5 \times 10^{12} \text{ s}^{-1}$. The probability of the dissociation of the axial Cr–CO bond is highly dependent on the excitation energy. The present study fully supports the general view that the overall course of photochemical processes is often determined by the events that take place at the earliest times after excitation, that is, within a few hundreds of femtoseconds, at most. This is especially true for the photochemistry of transition metal compounds, which have a high density of excited states with several possible reactive and relaxation channels open. The ultrafast branching of the evolution of the Franck–Condon excited state between the reactive and unproductive relaxation channels observed herein appears to be commonplace in organometallic photochemistry. It may well occur also in photochemical homolysis of metal–metal or metal–alkyl bonds.^{15,16,36} This underlines the importance of further ultrafast studies of organometallic photochemistry. As far as $\text{Cr}(\text{CO})_4(\text{bpy})$ is concerned, the characterization of decaying transients by picosecond time-resolved vibrational spectroscopy (IR or rR) is highly desirable. However, the complete understanding of its photochemistry, and of the reactivity of MLCT states at large, will require spectroscopic studies with a time resolution of tens of femtoseconds. Ideally, such studies should be complemented by quantum mechanical calculations of MLCT potential energy surfaces and of corresponding wave packet propagation. A qualitative model based on vibronic coupling between the ¹MLCT and ¹LF excited states along the dissociation coordinate has been proposed^{2,5,6} to account for the ultrafast CO dissociation from the MLCT excited state of $\text{Cr}(\text{CO})_4(\text{bpy})$ and other carbonyl diimine complexes of first-row transition metals. Indeed, the enabling role of a strongly avoided crossing between the ¹MLCT and ¹LF excited states for a prompt CO dissociation from MLCT states has recently been demonstrated by detailed quantum mechanical calculations of excited states of $\text{Cr}(\text{CO})_4(\text{bpy})$ and other carbonyl diimine complexes.^{31,39}

Acknowledgment. Dr. Mike Towrie and Dr. Anthony Parker of the CLRC Rutherford Appleton Laboratory are gratefully thanked for their technical assistance and stimulating discussions. We also thank EPSRC for the access to the CLRC Rutherford Appleton Laboratory facilities.

JA984350L

(35) Nijhoff, J.; Bakker, M. J.; Hartl, F.; Stufkens, D. J.; Fu, W.-F.; van Eldik, R. *Inorg. Chem.* **1998**, *37*, 661.

(36) Rossenaar, B. D.; van der Graaf, T.; van Eldik, R.; Langford, C. H.; Stufkens, D. J.; Vlček, A., Jr. *Inorg. Chem.* **1994**, *33*, 2865.

(37) Daniel, C.; Heitz, M. C.; Lehr, L.; Schroder, T.; Warmuth, B. *Int. J. Quantum Chem.* **1994**, *52*, 71.

(38) Finger, K.; Daniel, C.; Saalfrank, P.; Schmidt, B. *J. Phys. Chem.* **1996**, *100*, 3368.

(39) Guillaumont, D.; Daniel, C. *Coord. Chem. Rev.* **1998**, *177*, 181.

(31) Guillaumont, D.; Daniel, C.; Vlček, A., Jr. Manuscript in preparation.

(32) Manuta, D. M.; Lees, A. J. *Inorg. Chem.* **1986**, *25*, 1354.

(33) Iwata, K.; Hamaguchi, H. *J. Phys. Chem. A.* **1997**, *101*, 632.

(34) Hirata, Y.; Okada, T. *Chem. Phys. Lett.* **1991**, *187*, 203.